Detection of the X-ray spectra of imploding neon Z-pinch with elliptically bent mica crystal spectrometer

Jun Shi (施 军)[1], Shali Xiao (肖沙里)[1], Hongjian Wang (王洪建)[1], Xianbin Huang (黄显宾)[2], Libing Yang (杨礼兵)[2], and Shenye Liu (刘慎业)[3]

[1]*The Key Laboratory of Optoelectronic Technology and System, Ministry of Education, Chongqing University, Chongqing 400030*

[2]*Institute of Fluid Physics, China Academy of Engineering Physics, Mianyang 621900*

[3]*Research Center of Laser Fusion, China Academy of Engineering Physics, Mianyang 621900*

Received November 16, 2007

A wide variety of X-ray and extreme ultraviolet diagnostics are being developed to study on Yang accelerator. An elliptically bent crystal spectrometer is designed with a focal length of 1350 mm. A mica crystal with an interplanar spacing of 1.984 nm bent onto an elliptical substrate with eccentricity of 0.9485 is used. The crystal analyzer covers the Bragg angle range from 30° to 60°. The mica crystal can efficiently reflect radiation in multiple orders, covering the entire spectral range from 0.1 to 1.73 nm except for a gap from 0.86 to 1.0 nm. The application experiment is performed on Yang accelerator using the bent mica crystal analyzer. Spectra of neon-puff Z-pinch plasmas are recorded with a X-ray film, showing the H-like and the He-like lines of neon. Each spectrum has been identified and used for the wavelength calibration, and most of the line radiation is contained in the He-α and the L-α lines. The experimental results have demonstrated that the spectral resolution approximates 379.

OCIS codes: 300.6560, 350.5400, 340.0340.

doi: 10.3788/COL20080608.0622.

The hot and dense radiating plasmas produced in high power Z-pinch implosions have a wide variety of applications, ranging from materials testing and microscopy to the spectroscopy of highly charged ions[1,2]. A large number of high-temperature and high-density plasmas are produced by Z-pinch implosions, and the X-ray spectra emitted from them contain very abundant information, from which electron temperature and density can be induced[3−6]. In recent years, many spectrometers have been developed to measure X-ray spectra. The crystal spectrometer with natural and artifical crystal has become the most important tool for plasma diagnosis due to the simple structure, convenient operation, and low cost[7−10]. In this paper, an elliptically bent crystal spectrometer is described with a 0.9485 eccentricity, a 1350-mm focal length, and a $30° - 60°$ Bragg angle. It employs a mica crystal as the dispersive element and is equipped with an X-ray film mechanism as the spectral detector. Mica crystal can efficiently reflect radiation in multiple orders covering almost the entire spectral range from 0.1 to 1.73 nm. It is applied for X-ray diagnostics of Z-pinch plasmas on Yang accelerator.

The optical system was designed by the elliptical geometry, as shown in Fig. 1. The X-ray source is located at the front focal point F_1 (the center of the target chamber). The X-rays diffracted by the bent mica crystal are focused at the rear focal point F_2 where an exit slit is positioned. A 3-μm-thick aluminum foil is placed over the exit slit to cut off the visible light and low-energy X-ray. The X-ray film is effectively applied to measure X-ray spectra of a nanosecond source below the rear focal point F_2. In Fig. 1, F_1 and F_2 are the two focal points of an ellipse, θ is the Bragg diffracting angle, β is the spectral detection angle, R is the radius of the X-ray film. In the design of the spectrometer, the ellipse has an eccentricity of 0.9485 and a focal length (between the source and the center of the exit slit) of 1350 mm. The following expressions may be given by an elliptical equation,

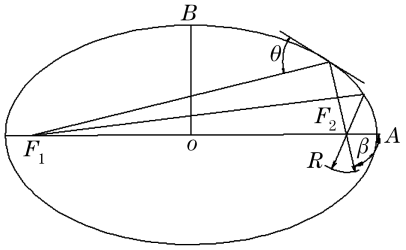

Fig. 1. Schematic of elliptically bent crystal spectrometer.

$$e = c/a, \tag{1}$$

$$b^2 = a^2 - c^2, \tag{2}$$

where a is the length of the long semiaxis, b is the length of the short semiaxis, c is the semifocal length, and e is the eccentricity. Using $e = 0.9485$, $c = 675$ mm, we can obtain $a = 711.65$ mm and $b = 225.43$ mm. Moreover, R is 50 mm, the arc length of the elliptical substrate is 128.27 mm.

The mica(002) crystal is used to diverge X-ray from the source, which is fixed on an elliptical-shape stainless-steel substrate with epoxy resin, the crystal is 125 mm in length, 10 mm in width, and 0.2 mm in thickness. The X-rays will be diffracted by the mica crystal when they arrive at the crystal plane. Crystal instrument obtain spectral resolution via the Bragg equation,

$$2d \sin\theta = n\lambda, \tag{3}$$

where $2d$ is the interplanar spacing, θ is the grazing angle relative to the crystal plane, n is the diffraction order,

Table 1. Spectral Range Covered by Each Reflection Order from a Mica Crystal

Order	I	II	III	IV	V
$\lambda_{\min}$ (nm)	0.992	0.496	0.331	0.248	0.198
$\lambda_{\max}$ (nm)	1.718	0.859	0.573	0.430	0.343
Order	VI	VII	VIII	IX	X
$\lambda_{\min}$ (nm)	0.165	0.142	0.124	0.110	0.099
$\lambda_{\max}$ (nm)	0.286	0.246	0.215	0.191	0.171

and λ is the X-ray wavelength. The spectral range is covered by each reflection order from a mica crystal ($2d = 1.984$ nm) for the range of grazing angles allowed by the experimental geometry ($30° - 60°$). Unlike many commonly used crystals, mica reflects efficiently in up to very high reflection orders, allowing us to simultaneously measure radiation in almost the entire range from 0.1 to 1.72 nm, except for a gap from 0.86 to 0.99 nm, as indicated by Table 1.

For this spectrometer, we utilize the first order bright stripe, by setting $n = 1$ we can obtain

$$\lambda = 2d \sin\theta. \tag{4}$$

Using Eq. (4) and $\theta = 30° - 60°$, the X-ray wavelength analyzed by the mica crystal is in the range of $0.992 - 1.718$ nm. We may relate the Bragg angle θ to the spectral detection angle β for the given elliptical geometry by[11,12]

$$\beta = \theta + \cos^{-1}\left(\frac{\cos\theta}{e}\right). \tag{5}$$

Substituting $e = 0.9485$ and $\theta = 30° - 60°$ into Eq. (5), the spectral detection angle is obtained as $\beta = 54.07° - 118.19°$.

The bent crystal spectrometer system is mainly composed of the dispersive element, the vacuum configuration, and the spectral detector. The dispersive element is a piece of mica crystal and the elliptical substrate is manufactured by using a computer-controlled milling machine to guarantee the satisfactory elliptical surface. The mica crystal is fixed on the elliptical surface with special slow-solidifying-rate epoxy resin. An exit slit is mounted on the bottom of the housing and its area is 8×20 (mm). A piece of aluminium foil is placed over the exit slit. The photo of the assembled spectrometer is shown in Fig. 2, where the bent crystal spectrometer system is bolted onto a 280-mm-diameter port of the Yang accelerator target chamber through the adapting flange and it is equipped with the X-ray film mechanism on the front port. In the spectrometer, the elliptical crystal analyzer is mounted on the steel plate and also replaced through the rear accessible port.

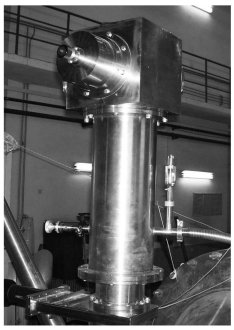

Fig. 2. Spectrometer system on Yang accelerator target chamber.

The experiments were performed on the Yang accelerator facility. Highly ionized Ne plasmas were formed by injecting about 100-μg/cm annular neutral gas columns into the 1.2×10^{-2}-Pa vacuum between the anode and cathode of the device, and the Yang accelerator was fired 1 μs after delivering, 1.0 MA at 1.0 MV to the load. The $\mathbf{J} \times \mathbf{B}$ force drives the plasmas inward at velocities near 5×10^7 cm/s. The plasmas stagnated on axis in 80 ns as the plasma kinetic energy is transferred to X-rays. The spectrometer was calibrated on the Yang accelerator target chamber and the emission spectra of neon plasmas were recorded with the X-ray film.

The X-ray spectra emitted from neon plasmas are shown in Fig. 3. Using a program edited in MATLAB in accordance with Eqs. (4) and (5), we identified in each spectrum the bright lines, as shown in Fig. 4. And we have used them for wavelength calibration. In addition to the brightest lines, there is a background, especially at higher energy that might be due to a Bremsstrahlung continuum and many unresolved lines originating from Ne IX high-n states ($n \geq 4$) which are not identified. A most striking observation from Fig. 4 is that about 80% of the line radiation from the neon plasmas is contained in the He-α and the L-α lines. The magnitude of these line widths can be correlated to electron temperature and density of the plasmas. A detailed analysis of the line profiles is in progress.

Table 2 summarizes the results of our measurements. Various Ne IX and Ne X transitions are identified and listed in the table. The experimental results have shown that the calculated spectral resolution ($\lambda/\Delta\lambda$) approximates 379 with $\Delta\lambda$ being the full-width at half-maximum (FWHM)[13].

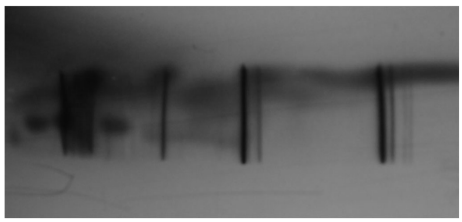

Fig. 3. Neon X-ray spectra measured with a bent crystal spectrometer.

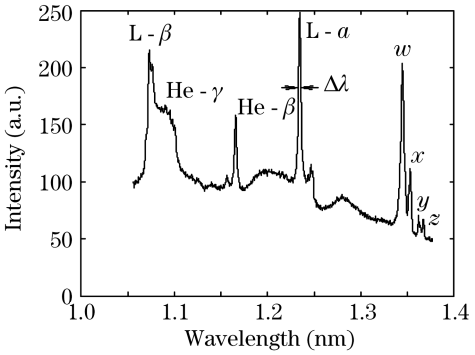

Fig. 4. Spectral intensity of neon emission.

Table 2. Ne IX and Ne X Transitions and Spectral Resolution

Label	Transition	λ (nm)	$\Delta\lambda$ (nm)	Resolution
He-α (z)	$1s2p\ ^3S_1$-$1s^2\ ^1S_0$	1.3761	–	–
He-α (y)	$1s2p\ ^3P_1$-$1s^2\ ^1S_0$	1.3618	–	–
He-α (x)	$1s2p\ ^3P_2$-$1s^2\ ^1S_0$	1.3529	0.0045	301
He-α (w)	$1s2p\ ^1P_1$-$1s^2\ ^1S_0$	1.3447	0.0043	312
He-β	$1s3p\ ^1P_1$-$1s^2\ ^1S_0$	1.1547	0.0031	372
He-γ	$1s4p\ ^1P_1$-$1s^2\ ^1S_0$	1.0760	–	–
L-α	$2p\ ^2P_{3/2}$-$1s\ ^2S_{1/2}$	1.2134	0.0032	379
L-β	$3p\ ^2P_{3/2}$-$1s\ ^2S_{1/2}$	1.0239	–	–

According to the elliptical focusing property, the optical system has been designed. The important optical parameters and spectrometer construction are also given. The experiment was performed on the Yang accelerator facility for testing the spectrometer. The X-ray spectra of neon plasmas showing the H-like and the He-like lines of neon were successfully recorded with X-ray film. Most of the line radiation is contained in the He-α and the L-α lines of neon. The experimental results have demonstrated that the spectral resolution of this spectrometer approximates 379.

This work was supported by the National Natural Science Foundation of China under Grant No. 10576041. The authors gratefully acknowledge the invaluable assistance of the staff operating Yang accelerator facility. J. Shi's e-mail address is gysj_001234@163.com.

References

1. A. Shlyaptseva, D. Fedin, S. Hamasha, C. Harris, V. Kantsyrev, P. Neill, N. Ouart, U. I. Safronova, P. Beiersdorfer, K. Boyce, G. V. Brown, R. Kelley, C. A. Kilbourne, and F. S. Porter, Rev. Sci. Instrum. **75,** 3750 (2004).
2. K. L. Wong, P. T. Springer, J. H. Hammer, C. A. Iglesias, A. L. Osterheld, M. E. Foord, H. C. Bruns, J. A. Emig, and C. Deeney, Phys. Rev. Lett. **80,** 2334 (1998).
3. B. L. Welch, H. R. Griem, and F. C. Young, J. Appl. Phys. **73,** 3163 (1993).
4. B. L. Welch, F. C. Young, and H. R. Griemb, J. Appl. Phys. **74,** 2260 (1993).
5. M. Bitter, K. W. Hill, B. Stratton, A. L. Roquemore, D. Mastrovito, S. G. Lee, J. G. Bak, M. K. Moon, U. W. Nam, G. Smith, J. E. Rice, P. Beiersdorfer, and B. S. Fraenkel, Rev. Sci. Instrum. **75,** 3660 (2004).
6. R. A. Nemirovsky, A. Ben-Kish, M. Shuker, and A. Ron, Phys. Rev. Lett. **82,** 3436 (1999).
7. R. Barnsley, N. J. Peacock, J. Dunn, I. M. Melnick, I. H. Coffey, J. A. Rainnie, M. R. Tarbutt, and N. Nelms, Rev. Sci. Instrum. **74,** 2388 (2003).
8. D. B. Sinars, G. R. Bennett, D. F. Wenger, M. E. Cuneo, and J. L. Porter, Appl. Opt. **42,** 4059 (2003).
9. S. Xiao, Y. Pan, X. Zhong, X. Xiong, G. Yang, Z. Liu, and Y. Ding, Chin. Opt. Lett. **2,** 495 (2004).
10. J. Gao, X. Zhong, X. Xiong, S. Xiao, and G. Yang, Chinese J. Lasers (in Chinese) **32,** 180 (2005).
11. B. L. Henke, H. T. Yamada, and T. J. Tanaka, Rev. Sci. Instrum. **54,** 1311 (1983).
12. X. Xiong, X. Zhong, S. Xiao, G. Yang, and J. Gao, Chin. Opt. Lett. **2,** 27 (2004).
13. J. Weinheimer, I. Ahmad, O. Herzog, H.-J. Kunze, G. Bertschinger, W. Biel, G. Borchert, and M. Bitter, Rev. Sci. Instrum. **72,** 2566 (2001).